

JPMTR-2103
DOI 10.14622/JPMTR-2103
UDC 004.93|51-3

Original scientific paper | 148
Received: 2021-03-22
Accepted: 2021-05-31

Image contrast enhancement using histogram equalization: a bacteria colony optimization approach

Saorabh Kumar Mondal¹, Arpitam Chatterjee² and Bipan Tudu³

¹Department of Instrumentation and Control Engineering,
Haldia Institute of Technology, Haldia, India

arpitam.chatterjee@jadavpuruniversity.in

²Department of Printing Engineering, Jadavpur University, Kolkata, India

³Department of Instrumentation and Electronics Engineering, Jadavpur University, Kolkata, India

Abstract

Histogram equalization (HE) is a popular method for image contrast enhancement that probabilistically maps the existing tonal levels of image to a new set of intensity levels. Despite simplicity, conventional global HE (GHE) has several limitations including visually disturbing false contouring, loss of original image features and wrong color representation in case of color images. Further modifications of GHE method have shown considerable improvement but many such techniques lack retention of original image characteristics. Computational intelligence algorithms can be a potential paradigm to address those limitations. This paper explores the scope of bacteria colony optimization (BCO) to obtain contrast enhancement while maintaining the original image characteristics. The fitness function has been formulated in frequency domain upon rigorous analysis in comparison with the results of existing contrast enhancement techniques. The paper includes implementation results with standard databases and the comparative evaluations. The comparative visual and objective evaluations confirm potential of BCO for improved performance.

Keywords: computational intelligence, Fourier analysis of contrast enhancement, image enhancement algorithm, image quality assessment

1. Introduction

Image contrast is an important characteristic of image that largely contributes towards perceived image quality. In general image contrast is the ratio between darkest and lightest part of the image. Contrast sensitivity has two major interpretations namely absolute and perceived contrast sensitivity. The former one is the minimum difference in luminance required for distinguishing between two intensities. The human eyes are not very sensitive to this and as a result very small difference may not be visible. The second one is more important as this is to which human eyes are sensitive. For instance, a bright object is more visible in a dark background than a bright one since the contrast between bright object and bright background is not enough for human eyes to distinguish. This phenomenon is mathematically modeled using contrast sensitivity function. There are interpretations called global and local contrast as well. The global contrast is an overall ratio between luminance of dark and light region of entire image while local contrast is the distin-

guishability of different image regions in reference to the luminance of its local surrounding pixels. Contrast enhancement techniques focus on perceived and local contrast. Due to many reasons, such as insufficient illumination, noise during image acquisition, information loss during image transmission and limitation in sensing capability of the optical sensors, low contrast images are resulted. Low contrast not only results in visual unpleasantness but also limits performance of different image analysis tasks like edge extraction, feature extraction and object recognition. Image contrast enhancement therefore is a key research area (Jayaraman, Esakkirajan and Veerakumar, 2011; Maini and Aggarwal, 2010).

The goal of image contrast enhancement is to reconstruct the low contrast input image with new intensity levels that keep informational symmetry with the original image. In the digital era histogram has evolved as a potential alternative to the gradation curves and differential operators of analog era. Histogram has several advantages as it provides intensity distribu-

tion across the available intensity levels as a numeric array. Different statistical information of the images can thus be derived from histograms that are widely used for many image processing and transformation operations like image compression, segmentation, etc. It provides better control over different visual regions in the images, i.e. shadow, mid-tone and highlight since it is a numerical array that provides clear brightness distribution across the local regions of the images. For instance, a narrow histogram conveys the low contrast since the pixel values can vary only within few intensities and rest of the intensity levels remain unutilized. Histogram can provide better insight of the image information particularly using the probability density function (*PDF*) which can also convey the gradient curve information when taken in the cumulative manner as cumulative *PDF* (*CPDF*). Being powerful and simple, histogram has become the obvious choice for many real-time applications of image reproduction and representation systems. Histogram equalization (HE) widens up the histogram of the input image across the available intensity levels since the histogram of low contrast images is found with narrow distribution.

The two broad categories of approaches towards contrast improvement are spatial intensity based and frequency-based approaches. Global histogram equalization (GHE) (Arici, Dikbas and Altunbasak, 2009) is one of the classical techniques under former class that maps the existing intensity levels to new levels that are more apart from each other resulting in better contrast. In GHE this is achieved probabilistically based on the *CPDF* of the image. The results of GHE frequently suffer from false contouring and artificial appearance. Many algorithms were proposed towards improvement over the conventional algorithm, for example brightness preserving bi-histogram equalization (BBHE) (Kim, 1997), dual sub-image histogram equalization (DSIHE) (Wang, Chen and Zhang, 1999), dynamic histogram equalization (DHE) (Abdullahal-Wadud, et al., 2007), exact histogram specification (EHS) (Coltuc, Bolon and Chassery, 2006), etc.

Adaptive histogram equalization (AHE) is another paradigm reported in this domain which can result in better enhancement in case of unevenly illuminated low-contrast images. Contrast limited adaptive histogram equalization (CLAHE) (Reza, 2004), overlapped sub-blocks and local histogram projection (NOSH) (Bovik, 2009), and fast local histogram specification (FLHS) (Liu, et al., 2014) are some of the examples of AHE. However, AHE can also cause artificial appearance in the enhanced images due to amplification of noise. Works have been reported towards suppression of noise which include a multi-level histogram segmentation based algorithm that can also achieve improvement in terms of noise suppression (Tohl and

Li, 2019) and pre-specified threshold based noise control in gain-controllable clipped histogram equalization (GC-CHE) (Kim and Paik, 2008). These algorithms involve contextual partitioning of the image prior to HE which provides a better sense of local mapping of the input gray levels.

In case of the approaches under the second group the images are converted to its frequency domain representations using appropriate transforms and then the contrast enhancement is performed in different frequency bands. Some of the examples in this category are logarithmic transform histogram matching (LTHM), logarithmic transform histogram shifting (LTHS), logarithmic transform histogram shaping using Gaussian distributions (LTHSG) (Cao, et al., 2018; Lin, et al., 2015; Agaian, Silver and Panetta, 2007), spatial entropy-based contrast enhancement (SECE) and spatial entropy-based contrast enhancement by discrete cosine transform (SECEDCT) (Celik, 2014). Residual spatial entropy-based contrast enhancement (RSECE) and its extension to discrete cosine domain (RSECEDCT) have been reported as an improvement over SECE (Celik and Li, 2016). Spatial mutual information rank (SMIRANK) is another algorithm proposed in recent years where the gray levels in images are considered as nodes that are subjected to PageRank algorithm for mapping and can achieve both local and global contrast enhancement simultaneously (Celik, 2016).

Retinex, a model that removes bias of source lighting from the image, has been adopted for contrast enhancement as well. It includes single scale, multi scale retinex (MSR) (Jobson, Rahman and Woodell, 1997) and adaptive MSR (AMSR) (Lee, et al., 2013) models. The application of camera response model has been reported in literature for contrast enhancement where exposure ratio map estimation is proposed towards assessment of the image under consideration as low-light image enhancement algorithm (LLIEA) (Ying, et al., 2017). The HE algorithms for image enhancement in specific applications have been developed as well. Improvement of infrared thermal image contrast based on the adaptive double plateaus HE (Li, et al., 2018), particle swarm optimization based infrared image contrast enhancement (Wan, et al., 2018), improvement of face images suffering from non-uniform illumination (Shakeri, et al., 2017) and dynamic contrast enhancement of magnetic resonance imaging (DCE-MRI) (Padhani, 2002) are few examples of application specific developments of HE.

In recent years computational intelligence (CI) algorithms have also been used to achieve contrast enhancement (Ritika and Kaur, 2013) where the mathematical formulations are used as an evaluation function, conventionally called fitness function (Osareh,

Shadgar and Markham, 2009; Zhang, et al., 2009). In this context application of artificial bee colony (ABC) has been reported where image contrast enhancement is modeled as a transfer function using incomplete beta function (IBF) (Chen, Li and Yu, 2016). Different applications of genetic algorithm (GA) for contrast enhancement can also be found (Tang, 2014) where the fitness function is developed using image intensity and edge information.

The application of hybrid approach involving ant colony algorithm, GA and simulated annealing to optimize the fitness function consisting of edge, intensity and entropy information has been reported as well (Hoseini and Shayesteh, 2010). Dynamic fuzzy histogram equalization (DFHE) technique has presented the application of fuzzy algorithms in this context (Sheet, et al., 2010). One of the attractive reasons of applying CI algorithms is their adaptive nature that has been proven advantageous over conventional methods in solving many critical engineering problems (Konar, 2006).

Bacteria colony optimization (BCO) is a popular CI algorithm (Passino, 2010; Chen, et al., 2014) that performs optimization using behavioral pattern on motile bacteria such as *Escherichia coli* (*E. coli*), *Salmonella* and *Myxococcus xanthus* (*M. xanthus*). In case of BCO the chemotaxis behavior of bacteria for surviving in the environment (such as nutrients) and their movement towards or away from a specific location is employed (Niu, et al., 2013). The rationale behind selecting BCO is its advantage of not largely being affected by the size and non-linearity of the problem. This algorithm also has advantages such as less computational time requirement and can handle higher number of objective functions when compared to the other evolutionary algorithms (Majumder, Laha and Suganthan, 2019). Yet this algorithm has not been applied for contrast enhancement to the best of our knowledge.

The contribution of this work is two-fold: mathematical formulation of a new objective function in frequency domain instead of using image quality evaluation metrics and optimizing the same using BCO. It is a tradeoff of spatial and frequency domain approaches since the objective function is formulated in spatial domain but the fitness evaluation is performed in frequency domain. A considerable number of test images, both grayscale and color ones, have been tested with the presented method. The performance comparison of the presented method is portrayed using subjective and objective evaluation measures. The subjective evaluation is supported by observations in frequency domain analysis. The objective evaluation is presented using different standard image quality assessment (IQA) metrics of both full reference (FR) and no-reference (NR) types.

2. Histogram equalization using bacteria colony optimization

2.1 Fitness function formulation

Histogram equalization in grayscale image is based on *CPDF* calculated from the image intensity values in spatial domain. In case of color images application of HE remains same however a conversion from the native RGB color space to a perceptual color space such as Hue, Saturation and Value (HSV) (Saravanan, Yamuna and Nandhini, 2016; Chien and Tseng, 2011) is needed. Applying the HE individually to the three channels of RGB can cause erroneous results because post HE mixing between the color channels can result in a totally different perceived color at output image. Hence conversion to a device independent color space like HSV is required prior to HE. After conversion the HE can be applied only to the Value (V) channel followed by combining the equalized V channel to the other two channels which remain unaltered. Finally image is reverted to RGB color space.

In this section a Fourier domain analysis on the results of histogram equalization techniques is presented towards development of fitness function. In this analysis the results of conventional and state-of-art techniques, namely, GHE, BBHE, DSIHE, CLAHE, AMSR and LLIEA have been included. These techniques represent different classes of algorithms as mentioned in previous section. The study can be described with the help of Figures 1 and 2 where the results of said algorithms, corresponding difference fast Fourier transform (FFT) spectra (original spectrum subtracted from the enhanced image spectrum) and projection plots (horizontal and vertical) of the FFT spectra have been included. It may be noted that the Fourier spectra have been processed to obtain a clear view of resulting changes. The processing here involves binarization of log-transformed FFT spectrum followed by morphological operation.

Figure 1 shows that most of the conventional techniques fail to retain the background of the test image while the advanced algorithms namely, CLAHE, AMSR and LLIEA can successfully retain that. The difference FFT spectra along with the projection plots can be a possible tool to analyze the results. In frequency domain the contrast enhancement is expected to introduce more frequency components and an expansion of the Fourier spectrum is desired for better results. But the expansion in Fourier spectrum should not be random. The contrast enhanced image is expected to generate the Fourier spectrum which will be an expanded or stretched version of the original image spectrum keeping parity to its shape of original image spectrum. Any HE algorithm that results in expansion of spectrum without keeping

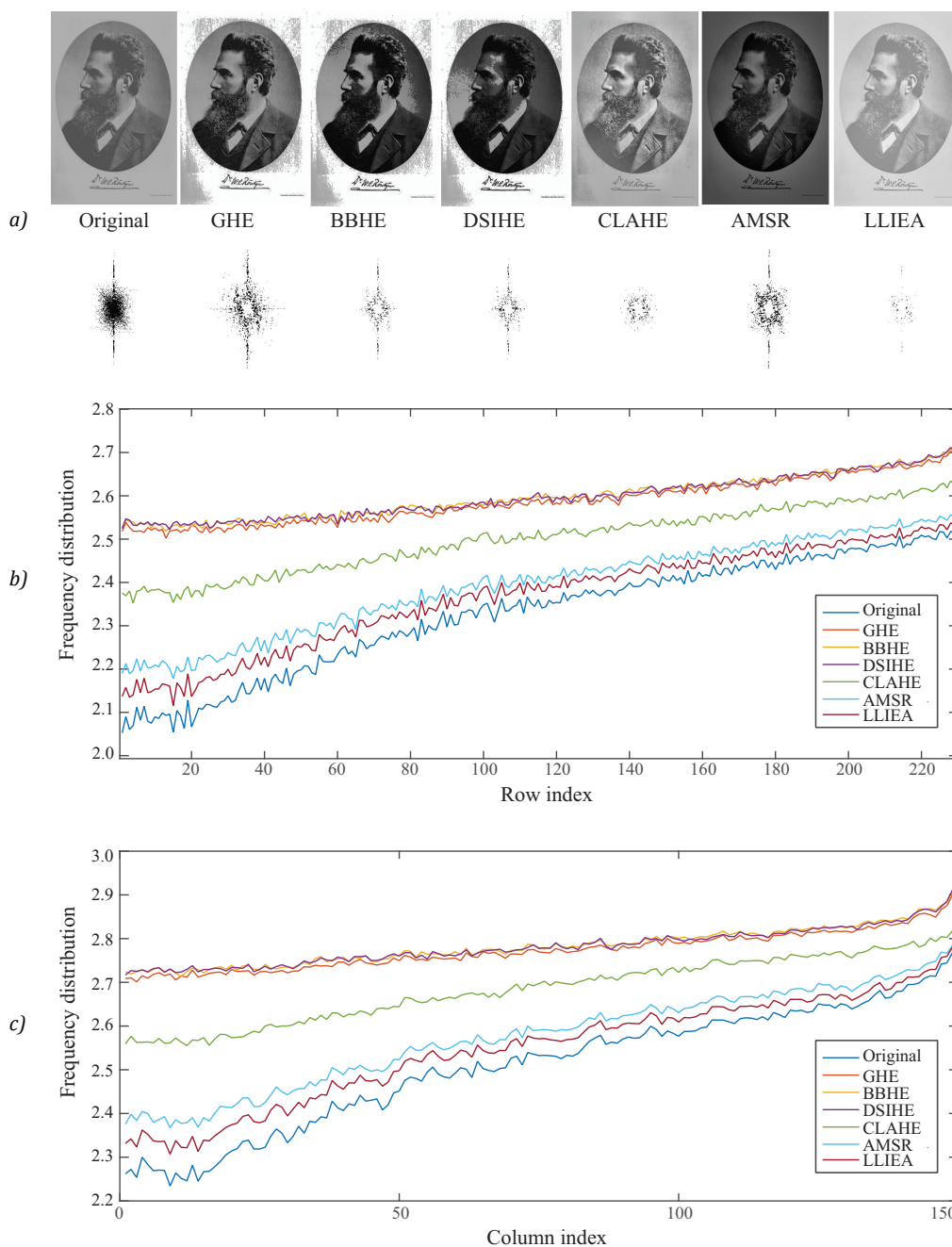


Figure 1: Fourier spectrum analysis of grayscale test image 'Man'; (a) results of different HE techniques and corresponding FFT spectra, (b) horizontal projection plots, and (c) vertical projection plots for different techniques

similarity to the shape of original spectrum will also show improvement but may not retain the important characteristics of the original image. As it can be seen in Figure 1, all classical HE enhancements result in contrast enhancement as reflected in their difference-spectrum by the resulted expansion. But at the same time expanded results are not well conforming to the shape of the original spectrum which results in loss of information as can be seen comparing the background gray region of original and modified images.

Hence, the algorithms can enhance image contrast or quality undoubtedly but there is noticeable lack in preserving the image characteristics. The projection plots can be possibly used to assess the shape conformance. The projection plots show that GHE, BBHE and DSIHE plots escalate through y axis keeping low adherence to the plot nature of original image. The plots for CLAHE shows comparatively better adherence while AMSR and LLIEA techniques are showing visibly improved adherence. These adherence results in better reten-

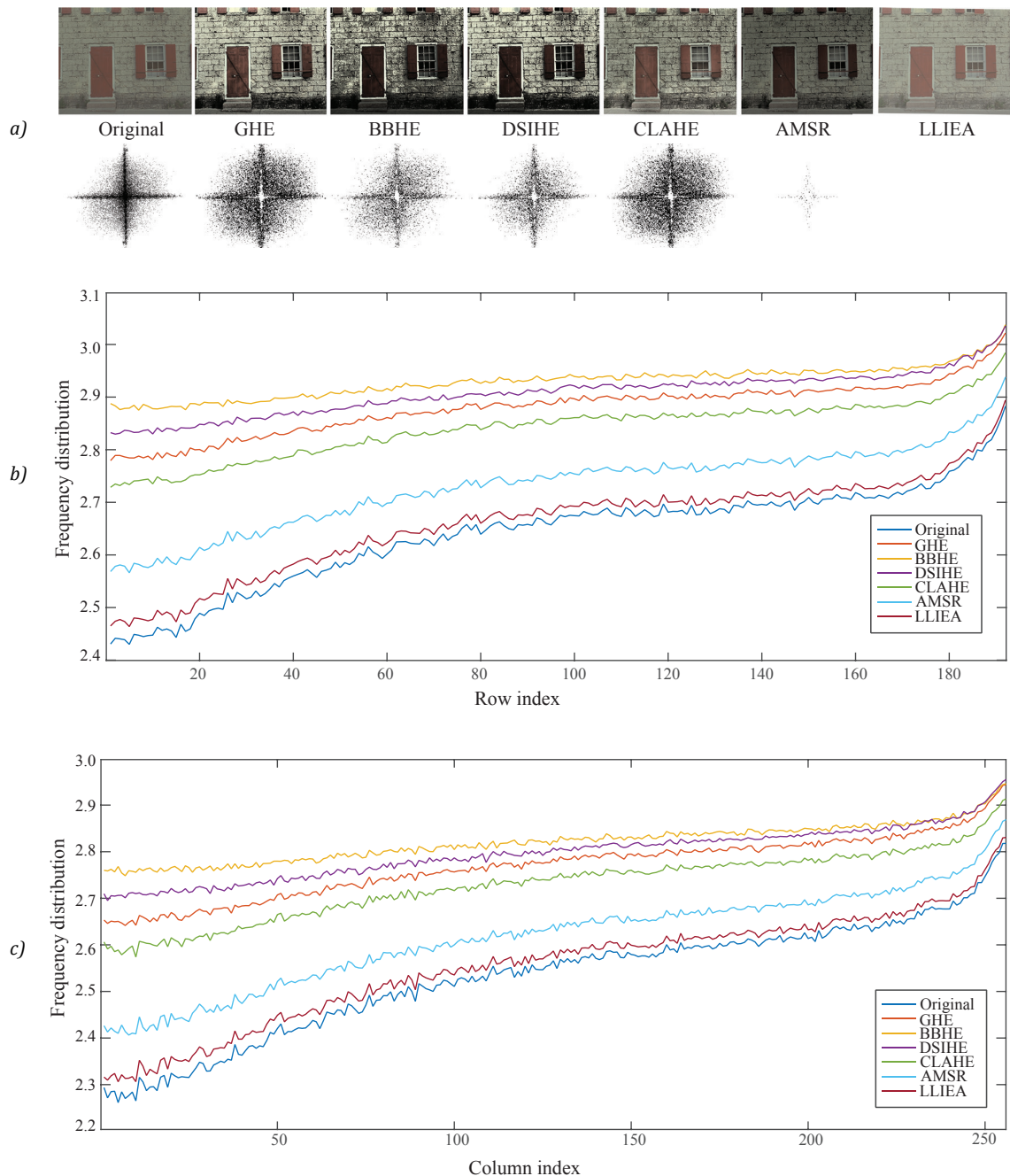


Figure 2: Fourier spectrum analysis of color test image 'House'; (a) results of different HE techniques and corresponding FFT spectra, (b) horizontal projection plots, and (c) vertical projection plots for different techniques

tion of original image features which can be seen by the retention of background grayness in their results. Nevertheless, the scope of improvements is still open. The same explanation may be drawn with color images as shown in Figure 2 where LLIEA does not show any visible expansion over the original image FFT spectra but it shows high degree of conformity to the shape of original image spectra as shown in projection plots of Figure 2. The classical techniques GHE, BBHE and DSIHE are more prone towards expansion of spectra

while less conforming to shape. The CLAHE method makes a balance between the expansion and shape conformity but a bit higher inclination towards spectra expansion while AMSR shows smaller expansion and better conformation to the shape.

From the presented images and the Fourier domain analysis it can be observed that the classical techniques are more towards the magnitude expansion than shape adherence while the advanced techniques attempt to

reach the balance between those two parameters but room of improvement is visible. The under- and over-enhancements can also be correlated to the magnitude expansion and shape adherence. Concretely, this work aims to achieve an optimum balance using BCO which can be a possible way to ensure avoidance of under- and over-enhancement problems that are visible in most of the classical as well as lately reported techniques. This leads to developing the optimization fitness function as a frequency domain parameter that will consider expansion and adherence to the shape of the original input spectrum. To use these parameters as fitness function the representative mathematical expression has been formulated as Equation [1].

$$\varphi = w_1 M \cdot w_2 S \quad [1]$$

where φ is the fitness function, M is the magnitude function and S is the shape parameter. The weight parameters w_1 and w_2 are tunable. The tuning of w_1 and w_2 is end-user requirement dependent; in the cases where retention of original image feature is of higher importance, such as in case of computer vision application, w_2 can be assigned with a higher value. In cases where the visual appearance is more important and loss of features may be compromised, for example, for reproduction operations like printing, w_1 can be assigned with a higher value. However, their sum must be equal to unity. Here, considering more general requirement, both visual appearance and feature retention have been given equal importance, i.e. $w_1 = w_2 = 0.5$.

In Equation [1], the magnitude function M can be calculated as the sum of the differences between processed FFT spectrum of original and enhanced image. It is important to note here that the expectation is towards expansion the magnitude function M not the contraction of the FFT spectrum. In the case of contraction the sum of the processed difference spectra becomes negative where the sum calculated from the binary difference image may be magnitude wise higher but with a negative difference value. This is not the desired case hence even if the value is higher this needs to have a measure of retreatment so that they are not favored over the case where a smaller positive value gets lower merit. To facilitate such cases the logarithmic value of sum is taken. Logarithmic transform can help in two ways: the range of the magnitude is reduced which gives ease of interpretation and also the contraction cases result in an imaginary value. In such cases the real value is divided by the imaginary value to get the final M value. The calculation of M value may be expressed as Equation [2].

$$M = \log(\sum D) \text{ where } D = HE_{\text{FFT}} - I_{\text{FFT}} \quad [2]$$

if $Im(M) \neq 0 : M = Re(M)/Im(M)$

where HE_{FFT} and I_{FFT} indicates the binary FFT spectra of histogram equalized image and original image, respectively. In Equation [2], Re and Im correspond to real and imaginary parts, respectively.

The shape parameter S in Equation [1] can be calculated from the projection plots shown in Figures 1 and 2 using the pair-wise Euclidian distance between the observations. Lower distance between observations interprets better adherence. The reciprocal combination of pair-wise distance in horizontal and vertical projections is considered in this work as shown in Equation [3]. The reason of taking reciprocal is to bring both S and M into same interpretability, i.e. for both of those parameters higher values indicate better results.

$$S = \frac{1}{\text{pair_dist}(I_{\text{hor}}, HE_{\text{hor}}) \cdot \text{pair_dist}(I_{\text{ver}}, HE_{\text{ver}})} \quad [3]$$

where, I_{hor} and HE_{hor} indicate the horizontal projections of original image and histogram equalized image, respectively. Similarly, I_{ver} and HE_{ver} represents the vertical projections. The higher value of M and S will cause a higher fitness value of φ which is considered as better fitness while performing the optimization.

2.2 Bacteria colony optimization

In BCO the bacterial behavior is mimicked. Like many other agent based search algorithms BCO also follows the dynamics of bacterial foraging to find an optimum solution of complex problem. Bacteria generally gather to the high nutrient areas by propelling themselves through rotation of the flagella maintaining an activity called chemotaxis (Chen, et al., 2014). The flagella rotate counter clockwise for forward movement; it is called that the organism “swims” or “runs”. When the flagella rotate clockwise, it causes the bacterium to “tumble” itself randomly and then it starts to swim again in a new direction. These *swim* and *tumble* activities help the bacterium for searching nutrients in random directions. Swimming and tumbling occurs more frequently for approaching a nutrient gradient by bacterium and to move away from some food for searching more foods. Bacterial chemotaxis is a complex combination of swimming and tumbling for placing the bacteria to a higher concentration of nutrients. Schematically BCO can be represented as an algorithm in Figure 3. The different mechanisms of BCO are described in following sections.

2.2.1 Chemotaxis

Chemotaxis mechanism works on the principle of *tumble* and *run* process. The movement of the i^{th} bacterium for every step of chemotactic process is expressed as Equation [4] (Niu, et al. 2013) considering $\theta^i(j, k, l)$

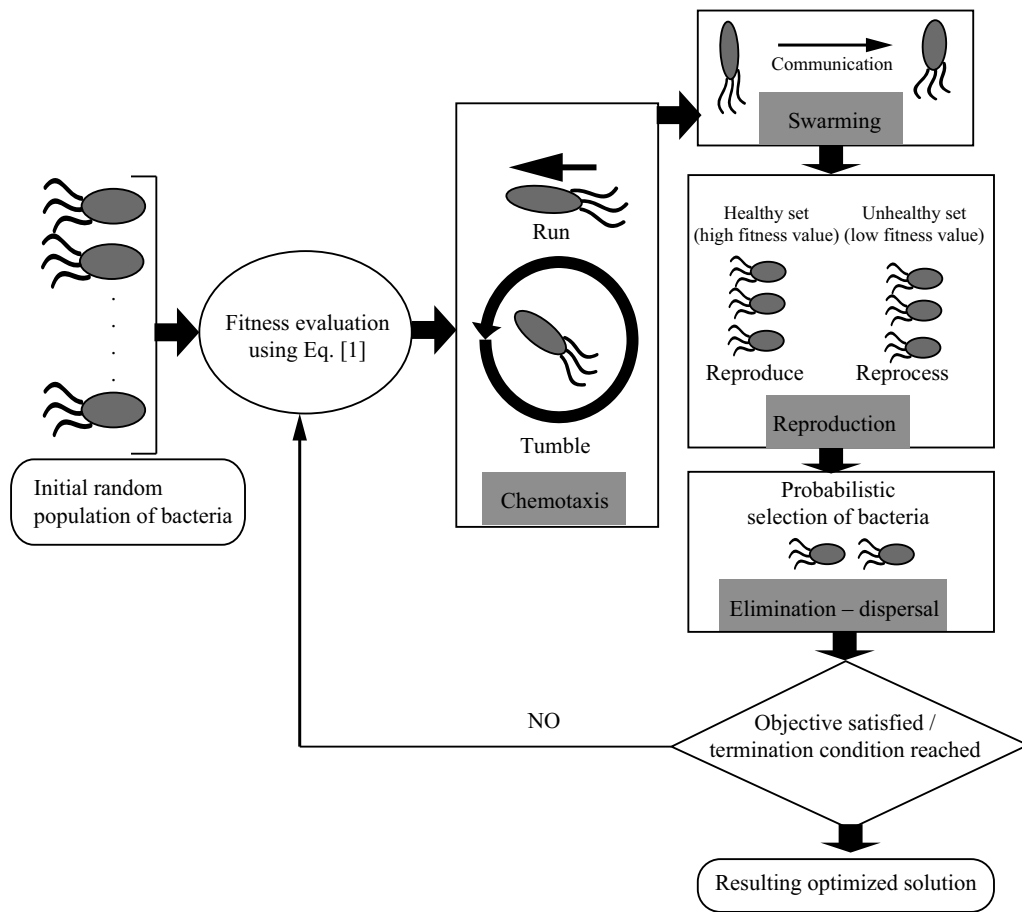


Figure 3: Schematic representation of BCO algorithm

denotes the position of i^{th} bacterium at j^{th} chemotactic, k^{th} reproductive, and l^{th} elimination-dispersal step. Further, $R(i)$ represents the step size of the chemotaxis for this bacterium at the time of every run or tumble (run-length unit).

$$\theta^i(j + 1, k, l) = \theta^i(j, k, l) + R(i) \frac{\Delta(i)}{\sqrt{\Delta^T(i) \cdot \Delta(i)}} \quad [4]$$

where $\Delta(i)$ is the j^{th} chemotactic step direction vector. At the time of run movement, $\Delta(i)$ is maintained the same with the last chemotactic step; otherwise, $\Delta(i)$ is a random vector whose elements are in the range of $[-1,1]$. Finally for each bacterium, a step fitness denoted by $J(i, j, k, l)$ is evaluated from the activity of run or tumble taken at each step of the chemotaxis process.

2.2.2 Swarming

Swarming mechanism as expressed in Equation [5] (Niu, et al., 2013) represents the the cell-to-cell communication process as each bacterium is capable of actuating, sensing, and decision-making mechanism. During the time of bacterium movement, it releases attractant

to provide indication of other bacteria to swarm that direction. In the meantime, every bacterium releases repellent to inform other bacteria to maintain a safe distance from it.

$$J_{cc}(\theta, P(j, k, l)) = \sum_{i=1}^{S_b} J_{cc}^i(\theta, \theta^i(j, k, l))$$

$$= \sum_{i=1}^{S_b} \left[-d_{attract} \exp \left(-w_{attract} \sum_{m=1}^{P_b} (\theta_m - \theta_m^i)^i \right) \right] \quad [5]$$

$$+ \sum_{i=1}^{S_b} \left[-h_{repellent} \exp \left(-w_{repellent} \sum_{m=1}^{P_b} (\theta_m - \theta_m^i)^2 \right) \right]$$

where, $J_{cc}(\theta, P(j, k, l))$ is the fitness function value with the addition of the actual fitness function for minimizing a presented time varying fitness function. The total bacteria number is denoted by S_b .

The number of parameters present in each bacterium to be optimized is denoted by P_b ; $w_{attract}$, $w_{repellent}$, $d_{attract}$ and $h_{repellent}$ are various optimization coefficients.

2.2.3 Reproduction

The reproduction mechanism maintains the good individual bacteria and eliminates bad ones based on the health condition of every bacterium. This is calculated by the sum of the step fitness during its life,

$$\text{i.e., } \sum_{j=1}^{N_c} J(i, j, k, l),$$

where N_c denotes the maximum number of steps in a chemotaxis process (Niu, et al., 2013). The fitness values of all bacteria are sorted in the order of good health status. In the production step, only the first half of total bacteria stay and second half of bacteria with poor health status are deleted. Each bacterium from the first half divides into two identical ones which are placed then in the same location to maintain the number of bacteria constant.

2.2.4 Elimination and dispersal

According to the change of environmental conditions, bacteria are greatly affected. In BCO model, when a certain number of reproduction processes happens, the dispersion processes occur. According to a fixed probability P_{ed} , some bacteria are to be selected for elimination and shift to another location within the environment. Simultaneously, the new ones are generated according to reproduction process.

2.3 Implementation of bacteria colony optimization in histogram equalization

This section presents the process of HE using BCO (HEBCO). To apply the BCO for color images first the image was converted to HSV color space from its native RGB color space. The V channel was separated and subjected to the BCO algorithm. The BCO was initiated with predefined numbers of solutions which are some randomly generated intensity levels in our case. Since the V channel values can vary from 0–255 in an 8-bit system the dimension of the space here is 256. The optimization has been performed towards maximization of the fitness function as described in section 2.1. Like all the meta-heuristics, BCO also is iterative in nature and the best solution at the end of each iteration is found using an objective function. This objective function can be kept same as fitness function but in our case an IQA based objective function has been used.

Considering our goal of retaining the original image features in enhanced image, brightness preservation is an important criteria and it can be measured using absolute mean brightness error (AMBE) (Raju, Dwarakish and Reddy, 2013) metric as expressed in Equation [6]. Apart from brightness, the optimization is driven to maintain information fidelity in terms

of image entropy (Wang and Ye, 2005) calculated as given in Equation [7] and structural similarity using structural similarity index measure (SSIM) (Horé and Ziou, 2010) calculated according to Equation [8].

$$AMBE(X, Y) = |E(X) - E(Y)| \quad [6]$$

where, X and Y denote the input image and output image, respectively, and E denotes the expected value of statistical mean. Lower AMBE indicates the better brightness preservation of the image.

$$ENT[P] = - \sum_k P_k \log(P_k) \quad [7]$$

where ENT denotes entropy and P is indicating the probability, which is the difference between two adjacent pixels of the image. Higher values of entropy indicate the richness of the image quality.

$$SSIM(X, Y) = l(X, Y) \cdot c(X, Y) \cdot s(X, Y) \quad [8]$$

where X and Y denote the input image and output image, respectively, and l denotes the luminance comparison of input and output image. Similarly, c and s denote the contrast and structural comparison between input and output image, respectively. Higher value of SSIM indicates better quality of output images. Using the above three parameters the objective function has been formulated as Equation [9]. The pseudo code of the HEBCO is presented in Table 1.

$$\emptyset = \frac{(ENT(I) + SSIM(I, O))}{AMBE(I, O)} \quad [9]$$

where I and O represent the enhanced image and original image, respectively. The \emptyset has been formulated such a way that a higher value will indicate better result. Thus, the objective of optimization is towards maximization. The algorithm performs iteratively with predefined termination condition. In this case the condition is either exhausting specified number of iterations or not showing any improvement for 10 consecutive iterations.

Table 1: Pseudo code of HEBCO

```

/* Assignment */
Load the low contrast image as input.
Initialize BCO parameters
  d: Dimension of the search space
  B: Number of bacteria
  Sc: Chemotaxis steps
  Ss: Swim steps
  Sre: Reproductive steps
  Sed: Elimination and dispersal steps
  Ped: Probability of elimination
  Rt: The run-length units during each run or tumble
Initialize random solutions based on input image histogram.

```

/* Update */

Compute the fitness value of these solutions using Equation [1].

Compute a new solution with improved fitness using the process of chemotaxis loop.

Store the fitness value for finding better value by run process of BCO operation.

Generate a number of random solutions based on the number of eliminating solutions by fitness value according to the process of reproduction loop and elimination–dispersal loop.

Compute the fitness of these randomly generated solutions.

Check the fitness value, whether it is better with respect to the previously selected solutions.

Store the fitness value and select the most-fit solutions.

Find the objective function value resulting from the most-fit solution at each iteration using Equation [9].

Terminate the loop while meeting the termination condition.

/* Enhancement */

Reconstruct the V channel with the best solution found using BCO.

Replace the original image V channel with the optimized V channel.

Convert the image back to RGB color space for visual presentation.

3. Results

The presented HEBCO was tested with different images from standard databases, namely, SIPI, TID2008 (TID), and LIVE (SIPI, n.d.; Ponomarenko, et al., 2009; Ghadiyaram and Bovik, 2015). The algorithms have been implemented using Matlab® software in Windows personal computer. All the images have been reproduced at 300 dpi resolution.

The experimental setup for the tunable parameters was arrived at using training–validation–testing method. To decide the parameter values a set of 100 images from different datasets was maintained. Images with all possible variations from the database were included in this dataset ranging from grayscale to color, different degree of low contrast and different illumination distortions. This dataset was partitioned in train, validation and test set with 60:20:20 proportions. The tunable parameters were varied within the ranges of values as commonly practiced in BCO. The combination that gave best fitness was considered for validation set. In validation set even lower range of variation with a smaller step size was used to finalize the parameter values. The final values arrived with the validation set are presented in Table 2 and were used for testing set as well as results presented in this paper.

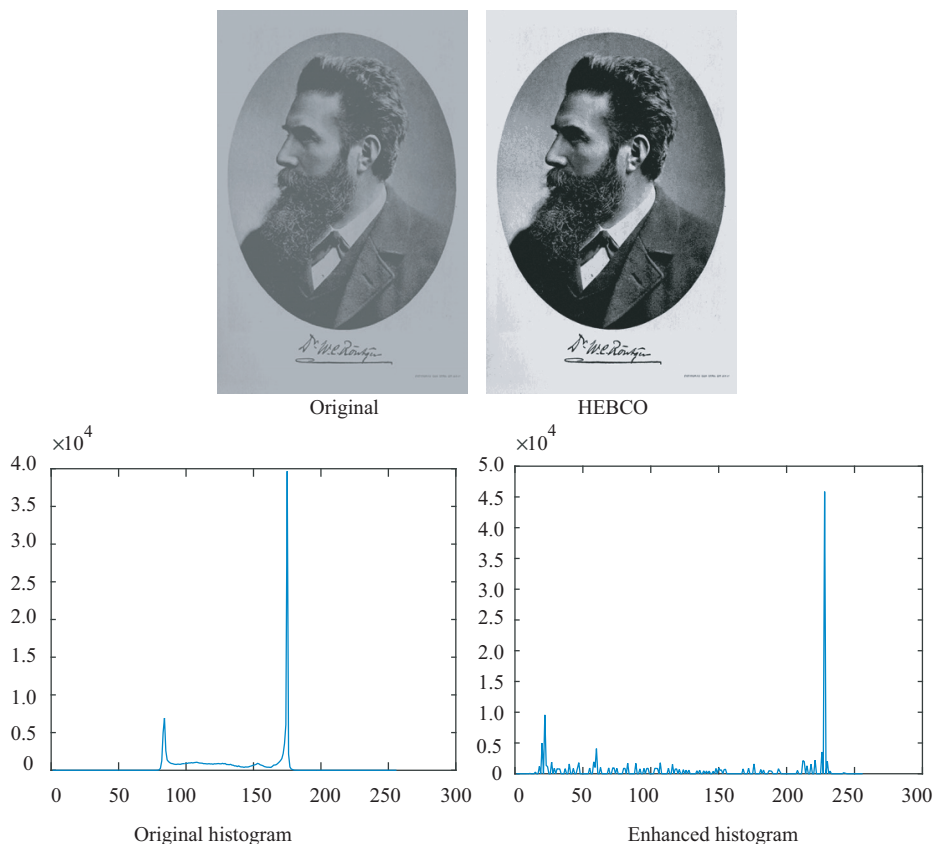


Figure 4: Result of HEBCO technique for grayscale test image 'Man'

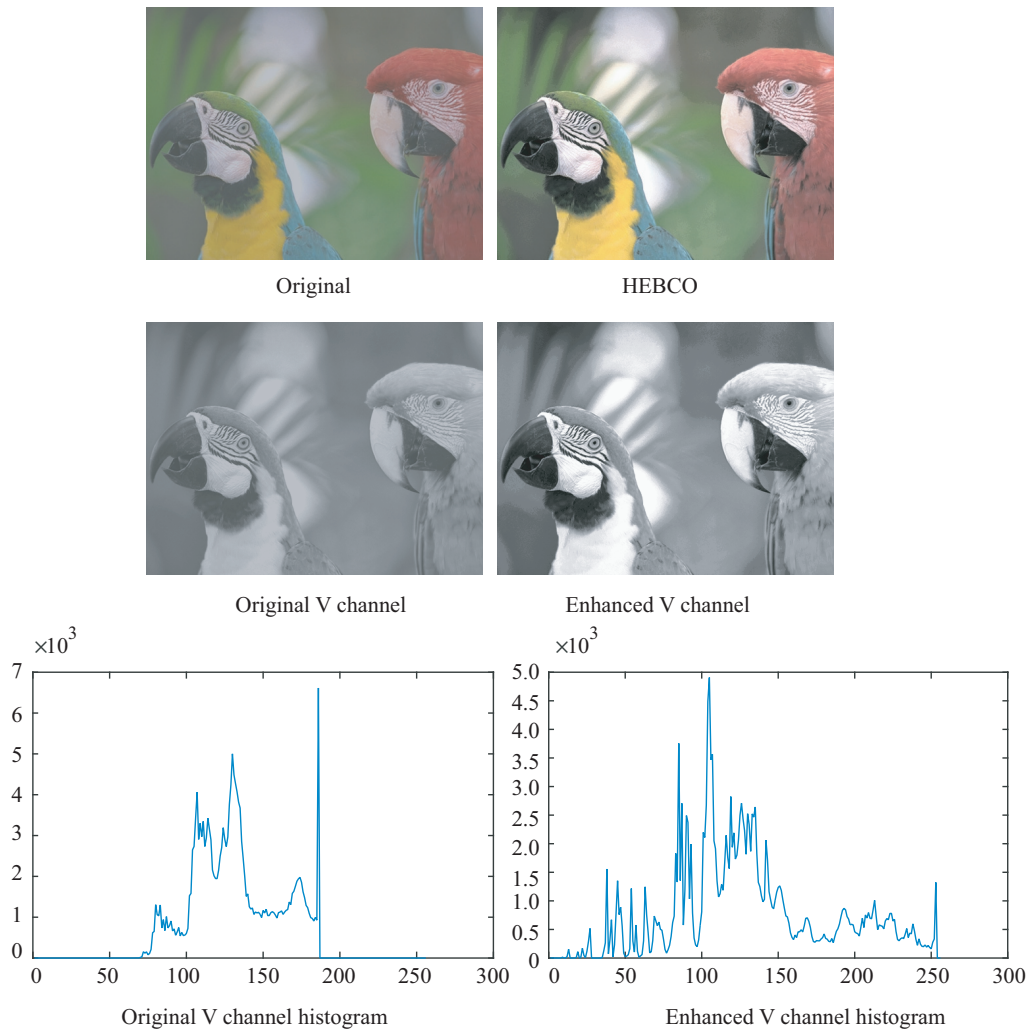


Figure 5: Result of HEBCO technique for color test image ‘Bird’

Table 2: HEBCO parameter setting

d : Dimension of the search space	256
B : Number of bacteria	10
S_c : Chemotaxis steps	50
S_{re} : Reproductive steps	8
S_{ed} : Elimination and dispersal steps	5
P_{ed} : Probability of elimination	0.20
R_l : The run-length units during each run/tumble	0.1

The results of HEBCO have been presented with two examples in Figures 4 and 5 for grayscale and color images, respectively. In both the cases histograms are included for understanding the contrast enhancement.

In Figure 4 it can be seen that HEBCO can retain the original image characteristics. The background grayness which many of the conventional as well as later developed HE techniques could not retain (as shown in Figure 1) has been well retained by HEBCO. There are

no visible false contouring and artificial patches in the HEBCO result. Also the balance between the dark and highlight regions is visually pleasant. The result also does not show occurrences of over- or under-exposure since the result is not inclined to white or black regions of intensity range. The corresponding histograms also convey the balanced enhancement. Another important observation in terms of histogram is retaining the peak information of original histogram.

Figure 5 shows the result with one of the color test images. In this case the corresponding V channels have also been included. It can be clearly seen that the contrast in the V channel has been significantly improved. That in turn results in improved visual appearance of enhanced image. The histograms of V channel convey that the HEBCO can result in stretching the original narrow histogram across the available intensity levels while maintaining the characteristics of original image histogram.

4. Discussions

This section presents the comparative assessment of HEBCO with the established reported techniques. Among different techniques, 10 have been considered in this paper. These techniques cover different paradigms of algorithms in both spatial and frequency domains.

Figure 6 shows the performance of different algorithms on a grayscale image. The enhancement capability of HEBCO is visibly better than the other techniques under consideration. The result of CLAHE is having higher sharpness while AGCWD provides higher smoothness and whiteness. Similarly, the AMSR and LLIEA results are under- and over-enhanced, respectively. The CI techniques based algorithms, except ABCHE, result in comparatively balanced enhancement.

Figures 7 to 9 are the examples of results with different algorithms on color test images. The visual appearances of HEBCO results clearly show the attainment of contrast improvement while retaining the original image characteristics in case of color images. In Figure 7 most of the conventional techniques fail to retain the color information of input image which is visible in case of leaves that are appearing almost black in the output

of most of the conventional techniques. While AMSR and DFHE results are showing the biasness of the level distribution towards dark intensities which causes under-enhancement, LLIEA and ABCHE show tendency of increasing overall whiteness which causes over-enhancement. The results of CLAHE, AGCWD, GAHE and HEBCO are more appealing but HEBCO shows better visual balance as tendency to increase whiteness and darkness can be seen in the results of AGCWD and GAHE, respectively. The observations drawn with Figure 7 remain true for Figure 8 as well but CLAHE shows a higher tendency of over-sharpening the image. In Figure 9 apart from previous observations one more important observation is the retention ability of patterns, particularly gradient. It can be seen that most of the techniques fail to retain the blue gradient pattern. In most of the cases the gradient is flattened down while HEBCO can retain that visibly.

Figures 10 and 11 are results from LIVE database images which consist of images captured by mobile devices in different lighting conditions and enhancement of contrast is challenging. It can be seen that all the CI algorithms perform well in this type of images. Conventional techniques like GHE, BBHE and DSIHE performs poorly in these cases and they tend to flatten down the images in either side of the intensity scale



Figure 6: Results of different HE techniques for grayscale test image 'Cat'; (top row from left to right) original (input) image, GHE, BBHE, DSIHE, (middle row left to right) CLAHE, AGCWD, AMSR, LLIEA, (bottom row left to right) DFHE, GAHE, ABCHE, and presented HEBCO

which causes patches, loss of details and poor visual appearance. The CLAHE, AGCWD, AMSR and LLIEA techniques can overcome those limitations but they also show under- or over-enhancement that can be seen as whitish appearance of LLIEA result or loss of desired brightness in AMSR result. The HEBCO result is comparatively better in terms of appearance since

there are no such patches or false contouring and also better retention of details as can be seen in the ‘denim’ hanging in the picture. In the results of conventional techniques the ‘denim’ pattern is almost turned into dark patches while CLAHE and HEBCO gives a much natural appearance along with contrast enhancement in the resulting image.



Figure 7: Results of different HE techniques for color test image ‘Flower’; (top row from left to right) original (input) image, GHE, BBHE, DSIHE, (middle row left to right) CLAHE, AGCWD, AMSR, LLIEA, (bottom row left to right) DFHE, GAHE, ABCHE, and presented HEBCO



Figure 8: Results of different HE techniques for color test image ‘Girl’; (top row from left to right) original (input) image, GHE, BBHE, DSIHE, (middle row left to right) CLAHE, AGCWD, AMSR, LLIEA, (bottom row left to right) DFHE, GAHE, ABCHE, and presented HEBCO

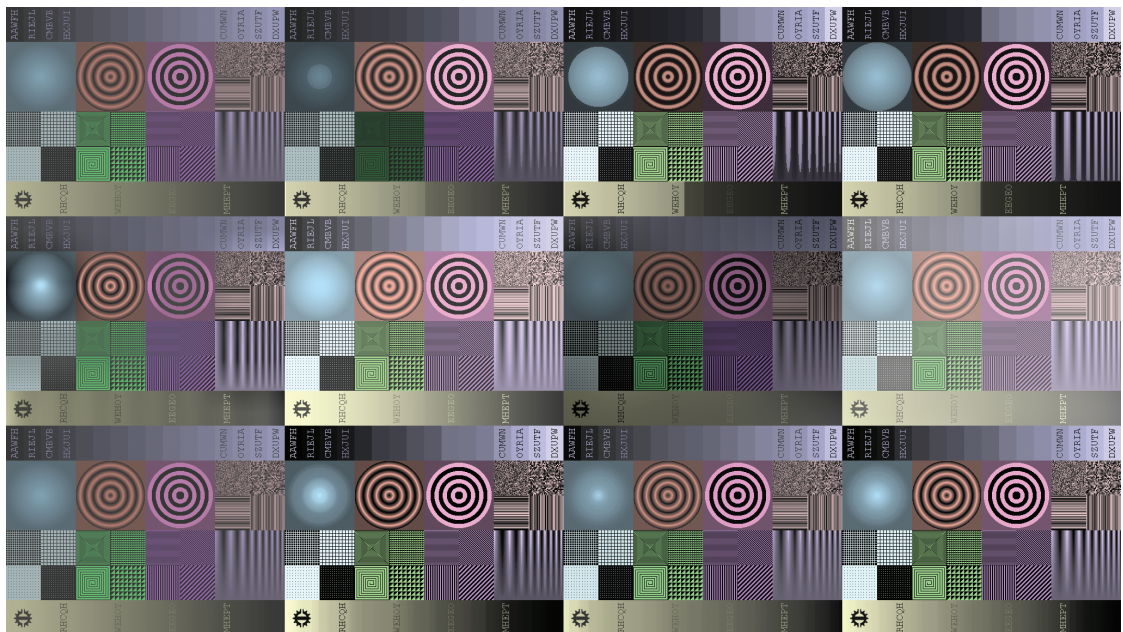


Figure 9: Results of different HE techniques for color test image 'Pattern'; (top row from left to right) original (input) image, GHE, BBHE, DSIHE, (middle row left to right) CLAHE, AGCWD, AMSR, LLIEA, (bottom row left to right) DFHE, GAHE, ABCHE, and presented HEBCO



Figure 10: Results of different HE techniques for color test image from LIVE database; (top row from left to right) original (input) image, GHE, BBHE, DSIHE, (middle row left to right) CLAHE, AGCWD, AMSR, LLIEA, (bottom row left to right) DFHE, GAHE, ABCHE, and presented HEBCO

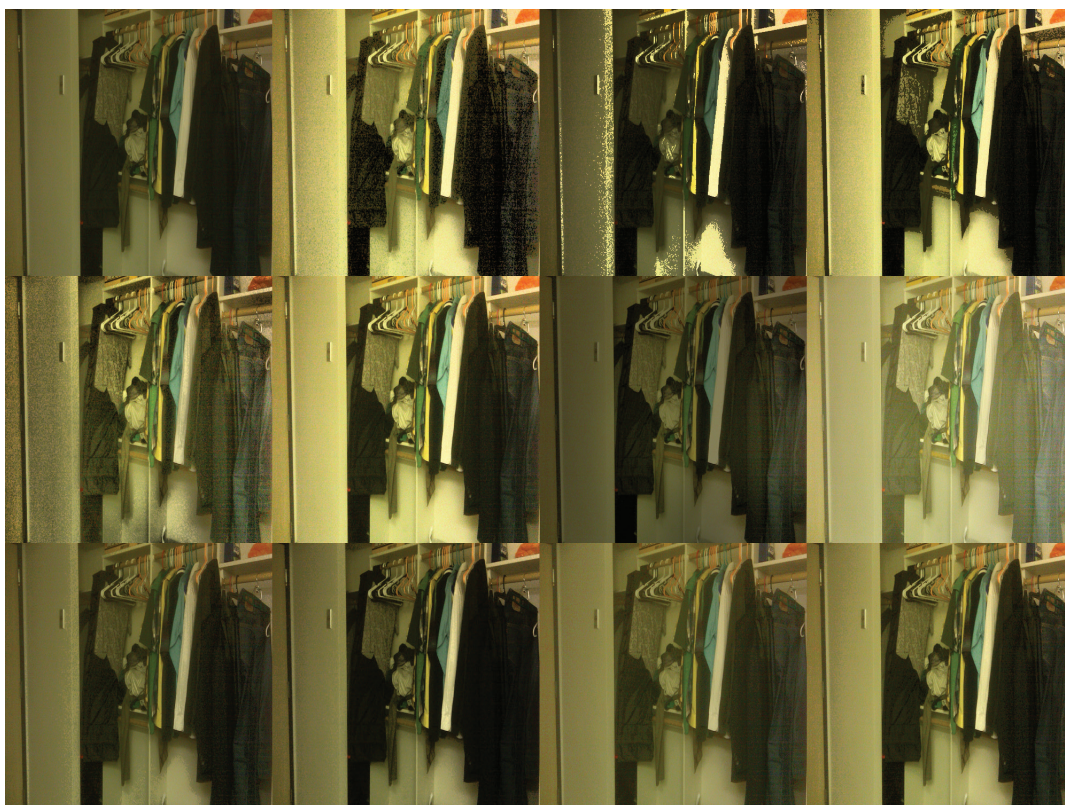


Figure 11: Results of different HE techniques for color test image from LIVE database; (top row from left to right) original (input) image, GHE, BBHE, DSIHE, (middle row left to right) CLAHE, AGCWD, AMSR, LLIEA, (bottom row left to right) DFHE, GAHE, ABCHE, and presented HEBCO

On an overall visual assessment it can be stated that CLAHE, AGCWD, AMSR and LLIEA techniques are superior to conventional HE techniques. But they also show limitations like over- or under-enhancement, unwanted sharpness or smoothness and loss of original image features. Such limitations can result in loss of naturalness in the enhanced images. The CI techniques show promising improvement on those parameters and HEBCO shows considerable potential by visually equivalent or better results in all the cases. The limitations can be further studied using the magnitude and shape parameters presented in this paper. A comparative presentation of the differential Fourier spectrum and projection plots with different techniques is presented in Figures 12 and 13. In those figures the algorithms have been classified into three groups for better visualization. The green lines present the algorithms that are based on histogram segmentation and statistical partitioning which include GHE, BBHE, DSIHE, CLAHE and AGCWD. The magenta lines plot model based algorithms that include AMSR and LLIEA. The blue lines indicate the CI based algorithms. To distinguish the original and the result of presented HEBCO, they have been represented using red and black color, respectively.

Figures 12 and 13 reveal interesting facts about the enhancement by different techniques. The DSIHE shows considerable magnitude expansion in spectra but like other histogram partitioning approaches it does not conform much to the original image brightness distribution pattern which can be seen in the green projections plots. The CLAHE and AGCWD are showing much better expansion in FFT spectra and conformity to the plots of original image including an escalation in the y -axis of the projection plots. The CLAHE and AGCWD plots are the plots coming in the region where the black, blue and magenta plots are coming. On the other hand AMSR and LLIEA results are showing good adherence to the original image features in the projection plots as the magenta plots are closely following the plot of original image and a reasonable escalation in the y -axis. All the CI based techniques show their potential to enhance the image contrast but HEBCO result shows visible adherence to the original image characteristics while improving the contrast. The difference FFT spectra are closely matching to the shape of original image spectra while in terms of projection plot it is neither going very high in the y -axis of the projection plots nor losing similarity to the original image plot. This confirms the potential

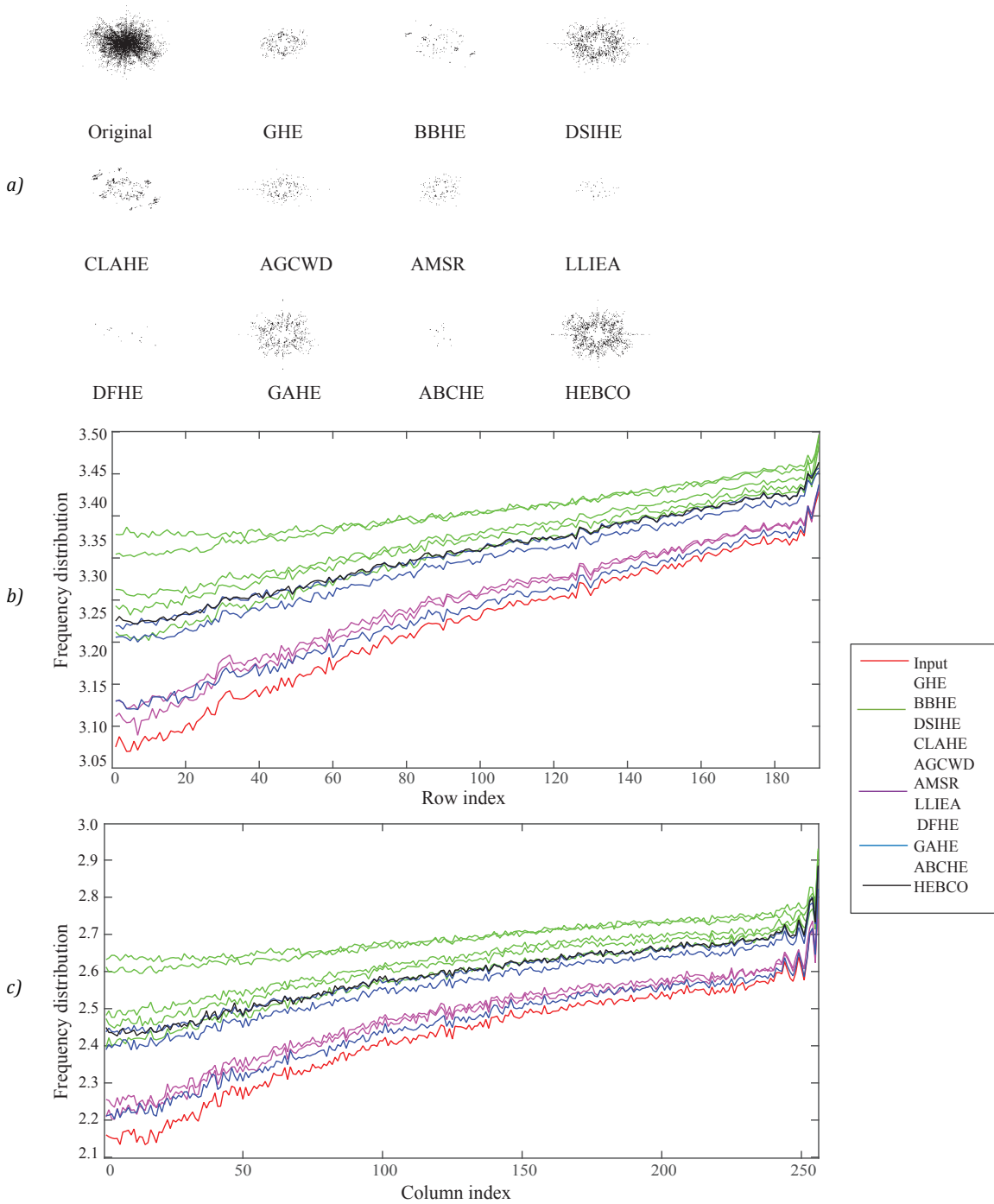


Figure 12: Adherence to the original image characteristics analysis for test image 'Girl' (a) differential magnitude spectra, (b) horizontal projection plots, and (c) vertical projection plots

of HEBCO to avoid over- or under-enhancements. The conventional GHE and BBHE in all the cases majorly increase the contrast keeping fewer adherences to the original image features as can be seen by the green plots appearing at the top, far away from the plot of original image, in the projection plots.

The visual analyses have further been extended to the objective evaluations against the IQA metrics. Among many IQA metrics in this work two FR and two NR metrics have been considered in this presentation. The FR (Larson and Chandler, 2010) metrics include the ground truth images for evaluation and in this paper

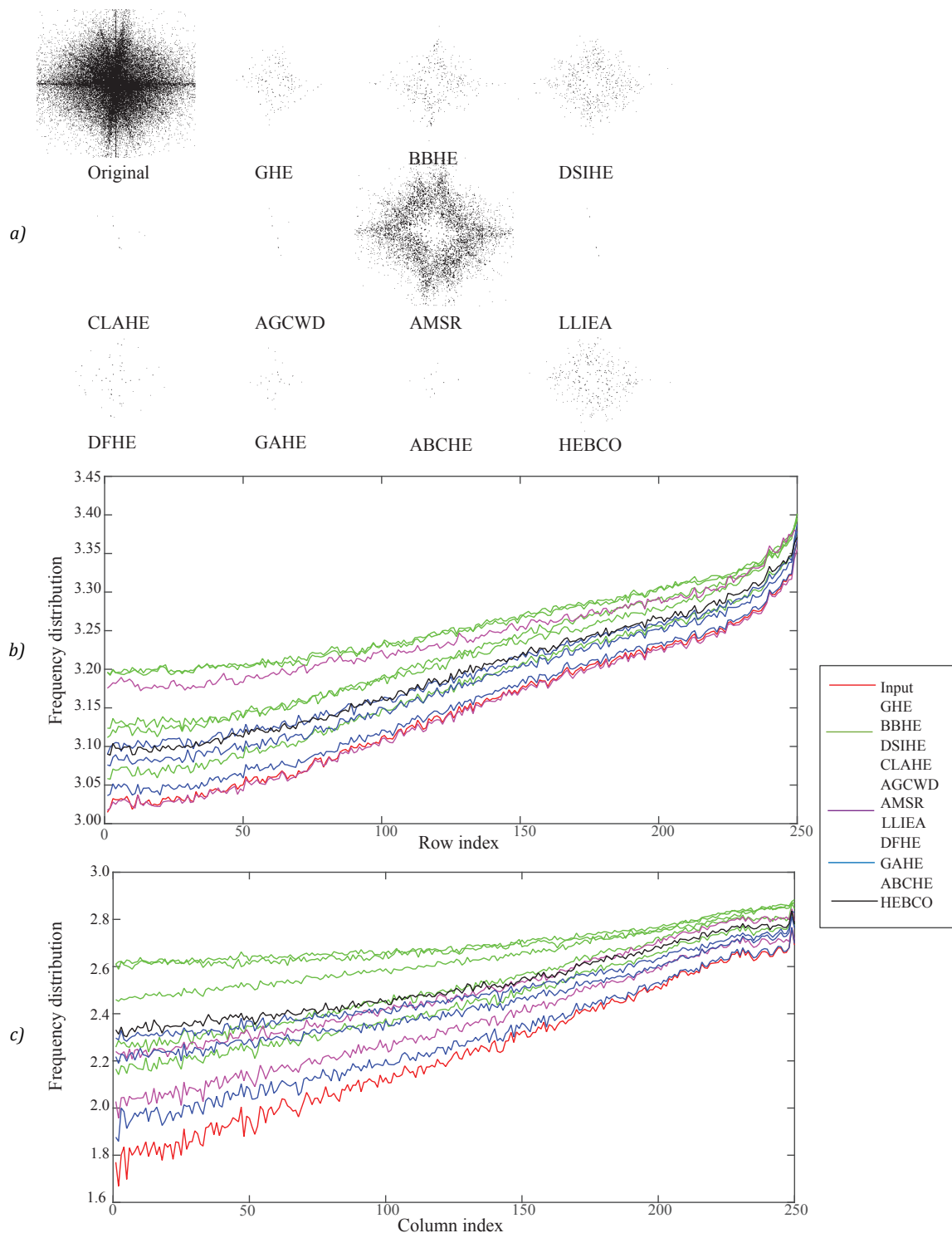


Figure 13: Adherence to the original image characteristics analysis for test image from LIVE database shown in Figure 11; (a) differential magnitude spectra, (b) horizontal projection plots, and (c) vertical projection plots semilogx scale

patch-based contrast quality index (PCQI) (Wang, et al., 2015) and feature similarity index measure (FSIM) (Zhang, et al., 2011) metrics have been used. The PCQI can be a good indicator of contrast enhancement and

local distortion measure while FSIM can be good measure for feature retention in enhanced images. Despite being FR metrics, both PCQI and FSIM consider the human perceptual characteristics in evaluation. The NR

(Mittal, Soundararajan and Bovik, 2012a) metrics do not include the ground truth for evaluation but they measure overall naturalness in enhanced images and a higher degree of naturalness is desired to avoid over- and under-enhancement causing artificial appearance in the enhanced images. The BRISQUE (Mittal, Moorthy and Bovik, 2011) and NIQE (Mittal, Soundararajan and Bovik, 2012b) are considered here as NR metrics for this purpose.

The PCQI is a metric popular in contrast enhancement evaluation. Instead of global enhancement it performs local patch based evaluation. It is based on signal decomposition philosophy and mathematically represented by variations in signal strength and signal structure as presented in Equation [10]. The outcome of PCQI can be interpreted in two ways; the PCQI map which is a graphical representation of contrast enhancement and a mean PCQI value which indicates improvement by higher values. The white and bright patches show improvement while the dark and black patches show degradation. For easier understanding PCQI map is often binarized setting patches with $PCQI < 1$ to 0 and rest to 1. There may be areas in output image which appear with high contrast and brightness but if that comes as a black patch in the binarized PCQI then it is showing under- or over-enhancement which results in distortions. Therefore, binarized PCQI map with lesser black patches indicates better enhancement. Similarly, calculating the mean value of patches as shown in Equation [10] the mean PCQI value is obtained which also has higher values for better enhancement. The binarized PCQI maps for two test images are shown in Figures 14 and 15.

$$PCQI(x, y) = q_i(x, y) \cdot q_c(x, y) \cdot q_s(x, y) \quad [10]$$

where, x and y are co-located patches in the reference image X and enhanced image Y , respectively, $q_i(x, y)$ is the difference estimation in terms of mean intensity, $q_c(x, y)$ is the parameter that corresponds to contrast change and for a better contrast image $q_c(x, y) > 1$. Finally, $q_s(x, y)$ corresponds to the structural distortion. If there are total N patches then mean PCQI is calculated as Equation [11].

$$PCQI(X, Y) = \frac{1}{N} \sum_{j=1}^N PCQI(x_j, y_j) \quad [11]$$

The PCQI maps shown in Figures 14 and 15 portray the potential of different algorithms towards enhancement and causing degradation in the resulting enhanced images. Figure 14 shows that BBHE, DSIHE and Ying et al. resulting considerable amount of distortion which we observed in terms of under-enhancement in our FFT spectrum and projection plot based analysis.

The distortions obtained in GHE, AGCWD and AMSR are comparable but they show higher degree of distortion than the DFHE, GAHE and ABCHE. The results of CLAHE and presented HEBCO are showing least degree of distortions in comparison to all other techniques. The results of PCQI in Figure 15 show that GHE produced higher degree of distortion like BBHE and DSIHE while DFHE produced lesser distortions. However, results of CLAHE and HEBCO are consistently maintaining visibly lesser amount of distortion. The AMSR and AGCWD show lesser distortion than LLIEA and all the CI techniques performed better. Experimental results have shown that CI algorithms work comparatively better in case of uneven illumination for the images from LIVE database.

The FSIM is a metric which can represent the feature similarity between reference/original and enhanced image. This can be calculated as Equation [12]. The higher values of FSIM indicate better results, i.e. better retention of original image features. It is based on phase congruency (PC) and gradient magnitude (GM) feature maps extracted between reference and enhanced images. The human perceptual nature is included in this metric in terms of phase congruent structure to which human eyes are sensitive. Feature retention can be important for computer vision applications of HE for example medical imaging.

$$FSIM = \frac{\sum_{x \in \Omega} S_L(x) \cdot PC_m(x)}{\sum_{x \in \Omega} PC_m(x)} \quad [12]$$

where Ω represents entire image in spatial domain, the similarity is measured between two images $f_1(x)$ and $f_2(x)$, $S_i(x)$ is the similarity calculated using PC and GM measures with assigned relative importance and $PC_m(x) = \max(PC_1(x), PC_2(x))$.

The BRISQUE is a convenient measure towards naturalness in the image. One advantage of BRISQUE is it does not include any frequency domain transforms like discrete cosine transform or wavelet transform as many other NR IQA techniques. This makes the metric simpler and faster. This metric is based on a generalized Gaussian distribution (GGD) fit of the mean subtracted contrast normalized (MSCN) coefficients applied on the locally normalized luminance of the input image. The scoring mechanism in the metric is based on a regression model where the singular value decomposition features have been subjected to support vector machine regressor (SVR). The lower scores indicate higher degree of naturalness in the image.

The NIQE is a feature based metric where a multivariate Gaussian (MVG) fit of the natural scene statistics (NSS) features are extracted from the test image



Figure 14: The binarized PCQI map of test image 'Girl'; (top row left to right) GHE, BBHE, DSIHE, CLAHE, (middle row left to right) AGCWD, AMSR, LLIEA, DFHE, (bottom row left to right) GAHE, ABCHE and HEBCO

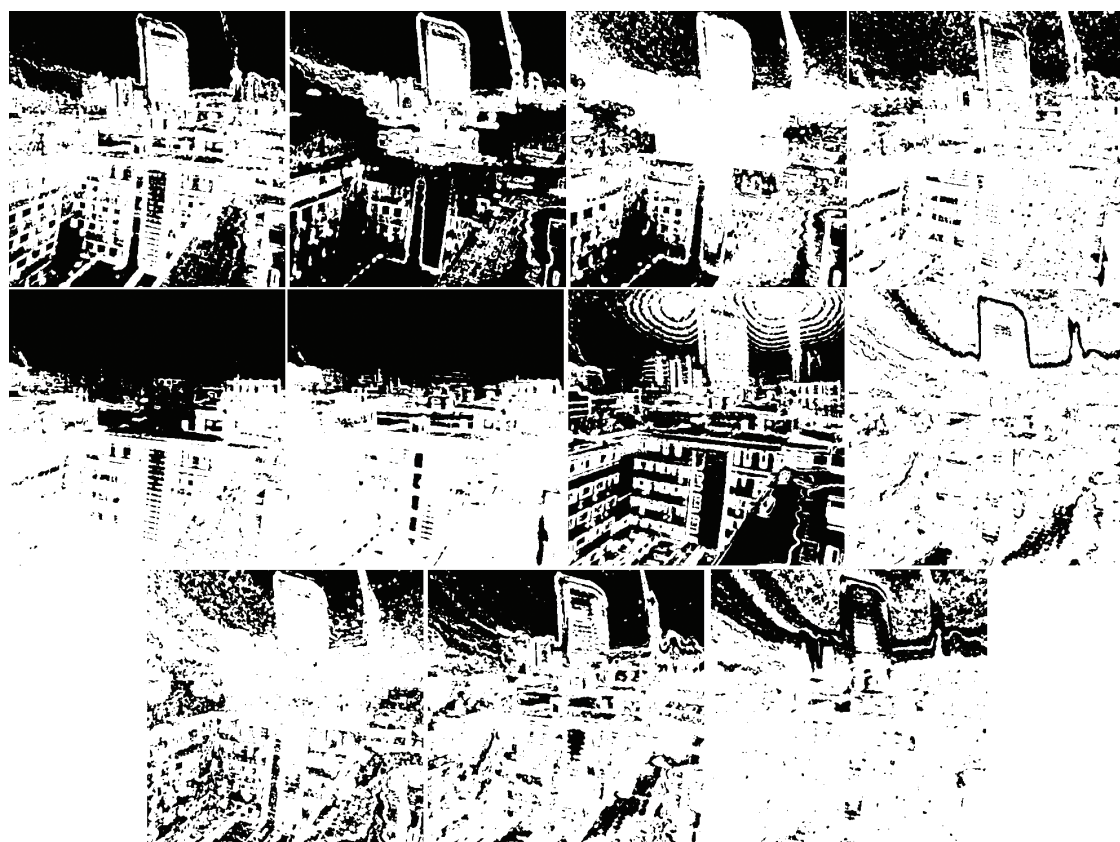


Figure 15: The binarized PCQI map of test image from LIVE database shown in Figure 10; (top row left to right) GHE, BBHE, DSIHE, CLAHE, (middle row left to right) AGCWD, AMSR, LLIEA, DFHE, (bottom row left to right) GAHE, ABCHE and HEBCO

and the quality is assessed as distance between this MVG and a defined MVG of the quality image features extracted from a numbers of natural images. A lower distance as indicated by lower metric value D indicates better result. It is expressed as Equation [13].

$$D(v_1, v_2, \Sigma_1, \Sigma_2) : \\ = \sqrt{\left((v_1 - v_2)^T \cdot \left(\frac{\Sigma_1 + \Sigma_2}{2} \right)^{-1} \cdot (v_1 - v_2) \right)} \quad [13]$$

where v and Σ are mean and covariance matrix, respectively, and T denotes the transpose operation. The natural MVG model and distorted MVG models are indexed as 1 and 2, respectively.

The mean evaluation results against these four metrics for individual databases are consolidated in Table 3 where the top two performers in respect to each metrics and databases have been highlighted. Table 3 shows that in terms of mean PCQI CLAHE performs best among all other techniques, HEBCO is next to CLAHE. But, in case of LIVE database, LLIEA performs better than CLAHE. The conventional techniques, particularly GHE, are also competitively performing for SIPI and TID databases but performance becomes visibly poor in case of LIVE database. This conveys the limitation of conventional techniques for unevenly illuminated images.

The significant downfall in the performance of DFHE is also visible while the CI techniques based HE perform consistently well against all the databases under consideration. Since, PCQI is a measure of patch-wise over- and under-enhancement or distortions in the obtained

image. It can be concluded from Table 3 that HEBCO can result in better contrast enhancement and lesser distortion in variety of images.

The FSIM is an indicator that can show the retention of original image features in resulting image. The LLIEA technique performs best across all the databases in this regard while HEBCO can perform well but could not perform as good as AMSR and DFHE in case of SIPI and TID databases, respectively. Although in case of LIVE database the performance is considerably better than most of the algorithms, which conveys the feature retention capability of HEBCO for unevenly illuminated images. In an overall judgment HEBCO performance is not poor as it can outperform many other techniques in terms of FSIM.

The BRISQUE and NIQE metrics convey the naturalness in resulting image which is very important and can be used to assess the ability of an algorithm to avoid artificial appearance caused due to inappropriate enhancements. In terms of those two metrics HEBCO shows its potential to retain naturalness in the resulting images avoiding under- and over-enhancement.

The conventional algorithms like GHE, BBHE and DSIHE along with some of the advanced algorithms like AMSR also cause loss of naturalness. LLIEA technique performs well against BRISQUE measure and AGCWD performs well in case of NIQE measure. Therefore, inference can be drawn that none of the techniques including HEBCO can perform best against all of the metrics but HEBCO has merits over many of the reported techniques in each aspect considered here. The HEBCO needs to improve its performance in terms of FSIM to secure position in top two best performers.

Table 3: Consolidated evaluation results against mean PCQI, FSIM, BRISQUE and NIQE

Techniques	mean PCQI			FSIM			BRISQUE			NIQE		
	SIPI	TID	LIVE	SIPI	TID	LIVE	SIPI	TID	LIVE	SIPI	TID	LIVE
GHE	1.018	1.156	0.466	0.702	0.608	0.622	33.8	19.16	84.18	6.68	3.6	19.64
BBHE	0.939	1.087	0.461	0.696	0.605	0.620	36.6	25.69	92.75	6.85	4.4	19.75
DSIHE	0.911	1.081	0.457	0.667	0.611	0.621	39.7	28.47	84.55	7.54	4.6	19.67
CLAHE	1.268	1.279	0.489	0.795	0.601	0.619	27.4	16.35	84.04	5.23	3.5	19.83
AGCWD	1.065	1.083	0.472	0.872	0.601	0.620	24.9	14.76	87.16	5.16	3.4	19.21
AMSR	0.977	0.999	0.878	0.928	0.927	0.300	29.7	14.57	94.79	20.20	19.4	22.40
LLIEA	0.999	0.999	0.999	0.929	0.924	0.997	21.9	11.61	86.72	19.90	19.1	19.26
DFHE	0.999	1.024	0.685	0.857	0.927	0.235	30.3	13.26	91.95	5.57	3.7	16.02
GAHE	1.022	1.105	0.973	0.881	0.599	0.978	28.2	14.68	20.37	5.34	3.5	16.17
ABCHE	0.944	1.096	0.907	0.885	0.879	0.976	28.5	8.92	17.63	5.68	3.5	16.33
HEBCO	1.083	1.164	0.974	0.904	0.883	0.978	23.6	11.40	18.02	4.97	3.4	15.23

5. Conclusions

The work has presented application of BCO towards contrast enhancement using HE methodology to obtain enhanced images while preserving the important characteristics of the original image. The frequency domain analysis of contrast enhancement has been used to formulate the fitness function and the optimization is performed in respect of different parameters like image brightness, signal/information fidelity and structural as well as feature information of the original image. The results have been presented visually and objective assessments have been drawn in comparison to the established HE techniques. The comparative analysis shows the competitive potential of HEBCO against the established techniques while overcoming different limitations of conventional HE approaches.

The work can further be extended to the application of other CI algorithms, tuning the fitness function for more robustness, BCO parameter optimization, a predictive model of the optimization framework where the input image can be enhanced based on a set of defined equalized histograms obtained by BCO, model based HE applications and inclusion of more optically derived measure of contrast for objective function formulation. The presented method has been explored considering image appearance in general which provides another important direction towards inclusion of prepress and press parameters in the objective function to obtain improved output quality of different prepress and printing systems. Finally, the paper has presented an important step towards application of BCO algorithms for image characteristics preserving contrast enhancement.

List of Abbreviations

ABC	artificial bee colony
AHE	adaptive histogram equalization
AMBE	absolute mean brightness error
AMSR	adaptive multi scale retinex
BBHE	brightness preserving bi-histogram equalization
BCO	bacteria colony optimization
CI	computational intelligence
CLAHE	contrast limited adaptive histogram equalization
<i>CPDF</i>	cumulative probability density function
DCE-MRI	dynamic contrast enhancement of magnetic resonance imaging
DFHE	dynamic fuzzy histogram equalization
DHE	dynamic histogram equalization
DSIHE	dual sub-image histogram equalization
EHS	exact histogram specification
<i>ENT</i>	entropy
FFT	fast Fourier transform
FLHS	fast local histogram specification
FR	full reference
FSIM	feature similarity index measure
GA	genetic algorithm
GC-CHE	gain-controllable clipped histogram equalization
GGD	generalized Gaussian distribution
GHE	global histogram equalization
GM	gradient magnitude
HE	histogram equalization
HE_{FFT}	binary FFT spectra of histogram equalized image
HSV	Hue, Saturation, Value
IBF	incomplete beta function
I_{FFT}	binary FFT spectra of original image
IQA	image quality assessment
LLIEA	low-light image enhancement algorithm
LTHM	logarithmic transform histogram matching
LTHS	logarithmic transform histogram shifting
LTHSG	logarithmic transform histogram shaping using Gaussian distributions
<i>M</i>	magnitude function
MSCN	mean subtracted contrast normalized coefficient
MSR	multi scale retinex
MVG	multivariate Gaussian
N_c	maximum number of step in a chemotaxis process
NOSHP	overlapped sub-blocks and local histogram projection
NR	no-reference
NSS	natural scene statistics
<i>P</i>	probability
P_b	bacterium parameter
PC	phase congruency
PCQI	patch-based contrast quality index
<i>PDF</i>	probability density function
RSECE	residual spatial entropy-based contrast enhancement
RSECDCT	residual spatial entropy-based contrast enhancement extension to discrete cosine domain
<i>S</i>	shape parameter
S_b	total bacteria number
SECE	spatial entropy-based contrast enhancement
SECDCT	spatial entropy-based contrast enhancement by discrete cosine transform
SMIRANK	spatial mutual information rank
SSIM	structural similarity index metric
SVR	support vector machine regressor
V	Value channel
φ	fitness function

References

- Abdullah-al-Wadud, M., Kabir, M.H., Dewan, M.A.A. and Chae, O., 2007. A dynamic histogram equalization for image contrast enhancement. *IEEE Transactions on Consumer Electronics*, 53(2), pp. 593–600. <https://doi.org/10.1109/TCE.2007.381734>.
- Agaian, S.S., Silver, B. and Panetta, K.A., 2007. Transform coefficient histogram-based image enhancement algorithms using contrast entropy. *IEEE Transactions on Image Processing*, 16(3), pp. 741–758. <https://doi.org/10.1109/tip.2006.888338>.
- Arici, T., Dikbas, S. and Altunbasak, Y., 2009. A histogram modification framework and its application for image contrast enhancement. *IEEE Transactions on Image Processing*, 18(9), pp. 1921–1935. <https://doi.org/10.1109/TIP.2009.2021548>.
- Bovik, A.C., 2009. *The essential guide to image processing*. 2nd ed. Boston, MA, USA: Academic Press.
- Cao, G., Huang, L., Tian, H., Huang, X., Wang, Y. and Zhi, R., 2018. Contrast enhancement of brightness-distorted images by improved adaptive gamma correction. *Computers & Electrical Engineering*, 66, pp. 569–582. <https://doi.org/10.1016/j.compeleceng.2017.09.012>.
- Celik, T., 2014. Spatial entropy-based global and local image contrast enhancement. *IEEE Transactions on Image Processing*, 23(12), pp. 5298–5308. <https://doi.org/10.1109/TIP.2014.2364537>.
- Celik, T., 2016. Spatial mutual information and page rank-based contrast enhancement and quality-aware relative contrast measure. *IEEE Transactions on Image Processing*, 25(10), pp. 4719–4728. <http://doi.org/10.1109/TIP.2016.2599103>.
- Celik, T. and Li, H.-C., 2016. Residual spatial entropy-based image contrast enhancement and gradient-based relative contrast measurement. *Journal of Modern Optics*, 63(16), pp. 1600–1617. <https://doi.org/10.1080/09500340.2016.1163427>.
- Chen, H., Niu, B., Ma, L., Su, W. and Zhu, Y., 2014. Bacterial colony foraging optimization. *Neurocomputing*, 137, pp. 268–284. <https://doi.org/10.1016/j.neucom.2013.04.054>.
- Chen, J., Li, C. and Yu, W., 2016. Adaptive image enhancement based on artificial bee colony algorithm. In: K. Hyunsung and L.-C. Hwang, eds. *Proceedings of the International Conference on Communication and Electronic Information Engineering (CEIE 2016)*. Guangzhou, China, 15–16 October 2016. <https://doi.org/10.2991/ceie-16.2017.88>.
- Chien, C.-L. and Tseng, D.-C., 2011. Color image enhancement with exact HSI color model. *International Journal of Innovative Computing, Innovation and Control*, 7(12), pp. 6691–6710.
- Coltuc, D., Bolon, P. and Chassery, J.-M., 2006. Exact histogram specification. *IEEE Transactions on Image Processing*, 15(5), pp. 1143–1152. <https://doi.org/10.1109/TIP.2005.864170>.
- Ghadiyaram, D. and Bovik, A.-C., 2015. *LIVE In the wild image quality challenge database*. [online] Available at: <<http://live.ece.utexas.edu/research/ChallengeDB/index.html>> [Accessed March 2021].
- Horé, A. and Ziou, D., 2010. Image quality metrics: PSNR vs. SSIM. In: *Proceedings of the 20th International Conference on Pattern Recognition*. Istanbul, Turkey, 23–26 August 2010. IEEE Computer Society. <https://doi.org/10.1109/ICPR.2010.579>.
- Hoseini, P. and Shayesteh, M.G., 2010. Hybrid ant colony optimization, genetic algorithm, and simulated annealing for image contrast enhancement. In: *Proceedings of the IEEE Congress on Evolutionary Computation (CEC)*. Barcelona, Spain, 18–23 July 2010. <https://doi.org/10.1109/CEC.2010.5586542>.
- Jayaraman, S., Esakkirajan, S. and Veerakumar, T., 2011. *Digital image processing*. New Delhi, India: Tata McGraw-Hill Education.
- Jobson, D.J., Rahman, Z. and Woodell, G.A., 1997. Properties and performance of a center/surround retinex. *IEEE Transactions on Image Processing*, 6(3), pp. 451–462. <https://doi.org/10.1109/83.557356>.
- Kim, T. and Paik, J., 2008. Adaptive contrast enhancement using gain-controllable clipped histogram equalization. *IEEE Transactions on Consumer Electronics*, 54(4), pp. 1803–1810. <https://doi.org/10.1109/TCE.2008.4711238>.
- Kim, Y.-T., 1997. Contrast enhancement using brightness preserving bi-histogram equalization. *IEEE Transactions on Consumer Electronics*, 43(1), pp. 1–8. <https://doi.org/10.1109/30.580378>.
- Konar, A., 2006. *Computational intelligence: principles, techniques and applications*. New Delhi, India: Springer Science & Business Media.
- Larson, E.C. and Chandler, D.M., 2010. Most apparent distortion: full-reference image quality assessment and the role of strategy. *Journal of Electronic Imaging*, 19(1): 011006. <https://doi.org/10.1117/1.3267105>.
- Lee, C.-H., Shih, J.-L., Lien, C.-C. and Han, C.-C., 2013. Adaptive multiscale retinex for image contrast enhancement. In: K. Yetongnon, A. Dipanda, R. Chebir, L. Gallo and N. Nain, eds. *SITIS'13: Proceedings of the International Conference on Signal-Image Technology & Internet-Based Systems*. Jaipur, India, 4–7 December 2013. Piscataway, NJ, USA: IEEE. <https://doi.org/10.1109/SITIS.2013.19>.
- Li, S., Jin, W., Li, L. and Li, Y., 2018. An improved contrast enhancement algorithm for infrared images based on adaptive double plateaus histogram equalization. *Infrared Physics & Technology*, 90, pp. 164–174. <https://doi.org/10.1016/j.infrared.2018.03.010>.

- Lin, S.C.F., Wong, C.Y., Rahman, M.A., Jiang, G., Liu, S., Kwok, N., Shi, H., Yu, Y.-H. and Wu, T., 2015. Image enhancement using the averaging histogram equalization (AVHEQ) approach for contrast improvement and brightness preservation. *Computers and Electrical Engineering*, 46(C), pp. 356–370. <https://doi.org/10.1016/j.compeleceng.2015.06.001>.
- Liu, H.-D., Yang, M., Gao, Y. and Cao, L., 2014. Fast local histogram specification. *IEEE Transactions on Circuits Systems for Video Technology*, 24(11), pp. 1833–1843. <https://doi.org/10.1109/TCSVT.2014.2329373>.
- Maini, R. and Aggarwal, H., 2010. A comprehensive review of image enhancement techniques. *Journal of Computing*, 2(3), pp. 8–13.
- Majumder, A., Laha, D. and Suganthan, P.N., 2019. Bacterial foraging optimization algorithm in robotic cells with sequence-dependent setup times. *Knowledge-Based Systems*, 172, pp. 104–122. <https://doi.org/10.1016/j.knosys.2019.02.016>.
- Mittal, A., Moorthy, A.K. and Bovik, A.C., 2011. *BRISQUE software release*. [online] Available at: <http://live.ece.utexas.edu/research/quality/BRISQUE_release.zip> [Accessed March 2021].
- Mittal, A., Soundararajan, R. and Bovik, A.C., 2012a. Making a ‘completely blind’ image quality analyzer. *IEEE Signal Processing Letters*, 20(3), pp. 209–212. <https://doi.org/10.1109/LSP.2012.2227726>.
- Mittal, A., Soundararajan, R. and Bovik, A.C., 2012b. *NIQE software release*. [online] Available at: <<http://live.ece.utexas.edu/research/quality/nique.zip>> [Accessed March 2021].
- Niu, B., Wang, H., Wang, J. and Tan, L., 2013. Multi-objective bacterial foraging optimization. *Neurocomputing*, 116, pp. 336–345. <https://doi.org/10.1016/j.neucom.2012.01.044>.
- Osareh, A., Shadgar, B. and Markham, R., 2009. A computational-intelligence-based approach for detection of exudates in diabetic retinopathy images. *IEEE Transactions on Information Technology in Biomedicine*, 13(4), pp. 535–545. <https://doi.org/10.1109/TITB.2008.2007493>.
- Padhani, A.R., 2002. Dynamic contrast-enhanced MRI in clinical oncology: current status and future directions. *Journal of Magnetic Resonance Imaging*, 16(4), pp. 333–483. <https://doi.org/10.1002/jmri.10176>.
- Passino, K.M., 2010. Bacterial foraging optimization. *International Journal of Swarm Intelligence Research*, 1(1), pp. 1–16.
- Ponomarenko, N., Lukin, V., Zelensky, A., Egiazarian, K., Carli, M. and Battisti, F., 2009. TID2008 – a database for evaluation of full-reference visual quality assessment metrics. *Advances of Modern Radioelectronics*, 10(4), pp. 30–45.
- Raju, A., Dwarakish, G.S. and Reddy, D.V., 2013. A comparative analysis of histogram equalization based techniques for contrast enhancement and brightness preserving. *International Journal of Signal Processing, Image Processing and Pattern Recognition*, 6(5), pp. 353–366. <http://doi.org/10.14257/ijisp.2013.6.5.31>.
- Reza, A.M., 2004. Realization of the contrast limited adaptive histogram equalization (CLAHE) for real-time image enhancement. *Journal of VLSI Signal Processing Systems for Signal, Image and Video Technology*, 38(1), pp. 35–44. <https://doi.org/10.1023/B:VLSI.0000028532.53893.82>.
- Ritika, and Kaur, S., 2013. Contrast enhancement techniques for images – a visual analysis. *International Journal of Computer Applications*, 64(17), pp. 20–25. <http://doi.org/10.5120/10727-5679>.
- Saravanan, G., Yamuna, G. and Nandhini, S., 2016. Real time implementation of RGB to HSV/HSI/HSL and its reverse color space models. In: *Proceedings of the IEEE International Conference on Communication and Signal Processing (ICCSP)*. Melmaruvathur, India, 6–8 April 2016. <http://doi.org/10.1109/ICCSP.2016.7754179>.
- Shakeri, M., Dezfoulian, M.H., Khotanlou, H., Barati, A.H. and Masoumi, Y., 2017. Image contrast enhancement using fuzzy clustering with adaptive cluster parameter and sub-histogram equalization. *Digital Signal Processing*, 62, pp. 224–237. <http://doi.org/10.1016/j.dsp.2016.10.013>.
- Sheet, D., Garud, H., Suveer, A., Mahadevappa, M. and Chatterjee, J., 2010. Brightness preserving dynamic fuzzy histogram equalization. *IEEE Transactions on Consumer Electronics*, 56(4), pp. 2475–2480. <http://doi.org/10.1109/TCE.2010.5681130>.
- SIPI, n.d. *The USC-SIPI image database*. [online] Available at: <<http://sipi.usc.edu/database/>> [Accessed March 2021].
- Tang, L., 2014. Image edge detection based on quantum genetic algorithm. *Computer Modeling & New Technologies*, 18(12B), pp. 517–523.
- Tohl, D. and Li, J.S.J., 2019. Contrast enhancement by multi-level histogram shape segmentation with adaptive detail enhancement for noise suppression. *Signal Processing: Image Communication*, 71, pp. 45–55. <https://doi.org/10.1016/j.image.2018.10.011>.
- Wan, M., Gu, G., Qian, W., Ren, K., Chen, Q. and Maldague, X., 2018. Particle swarm optimization-based local entropy weighted histogram equalization for infrared image enhancement. *Infrared Physics & Technology*, 91, pp. 164–181. <https://doi.org/10.1016/j.infrared.2018.04.003>.
- Wang, C. and Ye, Z., 2005. Brightness preserving histogram equalization with maximum entropy: a variational perspective. *IEEE Transactions on Consumer Electronics*, 51(4), pp. 1326–1334. <https://doi.org/10.1109/TCE.2005.1561863>.
- Wang, S., Kede, M., Yeganeh, H., Wang, Z. and Lin, W., 2015. A patch-structure representation method for quality assessment of contrast changed images. *IEEE Signal Processing Letters*, 22(12), pp. 2387–2390. <https://doi.org/10.1109/LSP.2015.2487369>.

- Wang, Y., Chen, Q. and Zhang, B., 1999. Image enhancement based on equal area dualistic sub-image histogram equalization method. *IEEE Transactions on Consumer Electronics*, 45(1), pp. 68–75. <https://doi.org/10.1109/30.754419>.
- Ying, Z., Li, G., Ren, Y., Wang, R. and Wang, W., 2017. A new low-light image enhancement algorithm using camera response model. In: *Proceedings of 2017 IEEE International Conference on Computer Vision Workshops (ICCVW)*. Venice, Italy, 22–29 October 2017. Piscataway, NJ, USA: IEEE. <https://doi.org/10.1109/ICCVW.2017.356>.
- Zhang, G., Sun, D., Yan, P., Zhao, H. and Li, Z., 2009. A LDCT image contrast enhancement algorithm based on single-scale retinex theory. In: M. Mohammadian, ed. *Proceedings of the IEEE International Conference on Computational Intelligence for Modeling Control & Automation*. Vienna, Austria, 10–12 December 2008. Piscataway, NJ, USA: IEEE. <https://doi.org/10.1109/CIMCA.2008.231>.
- Zhang, L., Zhang, L., Mou, X. and Zhang, D., 2011. FSIM: a feature similarity index for image quality assessment. *IEEE Transactions on Image Processing*, 20(8), pp. 2378–2386. <https://doi.org/10.1109/TIP.2011.2109730>.